

Design of High Gain Corrugated Antipodal Vivaldi Antenna With π Shaped Metamaterial for SATCOM Applications

Nitin Muchhal*, Mostafa Elkhoully, Yaarob Fares, Renato Zea Vintimilla
Fraunhofer Institute for Integrated Circuits IIS, Am Wolfsmantel 33, 91058 Erlangen, Germany
{firstname.lastname@iis.fraunhofer.de}

*Corresponding author e-mail: nmuchhal@gmail.com

Abstract— A wideband and high gain corrugated epsilon negative index metamaterial (ENG) Antipodal Vivaldi Antenna (AVA) with gain >12 dBi and working in frequency range from 10 GHz - 25 GHz (for SATCOM applications) is proposed in this paper. The overall performance of the proposed AVA is enriched by using a triangular shaped corrugation slots and π (π) shaped epsilon negative metamaterial cells. The ' π ' shaped metamaterial unit cells are positioned on the upper surface amid both radiators of AVA to emanate the intense electric field in the end-fire direction. The proposed antenna size is 22.6 mm \times 15.8 mm \times 1.6 mm and it is designed on the FR4 substrate. The maximum gain of the antenna is 12.2 dBi at 14.5 GHz.

Keywords- Metamaterial; Corrugation; Antipodal Vivaldi Antenna (AVA); Gain; SATCOM.

I. INTRODUCTION

To accomplish pervasive connectivity on the globe, SATellite COMmunication (SATCOM) is a crucial constituent of next-generation wireless communications. In recent times, a significant amount of research work has been proposed to design various vital components [1][2] for SATCOM applications. The Vivaldi antenna was proposed and designed by Gibson for high-frequency applications [3]. Later, Gazit improved it by giving it an antipodal shape to enhance the bandwidth and gain [4]. By incorporating numerous enhancement methods e.g., adding parasitic patch, dielectric lens, array and metamaterial, the parameters of the Antipodal Vivaldi Antenna (e.g., directivity, bandwidth, reduction inside lobe level etc.) can be improved. In [5], a parasitic patch of elliptical shape is used to increase the directivity of the Antipodal Vivaldi Antenna (AVA), but it has the drawback of bigger size. The dielectric lens used in [6] upsurges the end-fire radiations, but at the cost of a large size. The AVA Array design proposed by [7] increases the gain but suffers from augmented mutual coupling due to proximity of antenna elements. Amongst several techniques, the enhancement technique using metamaterial is quite effective without increasing the size of an antenna. After an intensive literature review, it is established that little work is done on AVA with metamaterial for SATCOM applications. This paper presents a compact and enhanced gain AVA with ' π ' (π) shaped metamaterial for SATCOM applications.

The rest of the paper is structured as follows. Section II elaborates on the design of the proposed conventional AVA. Section III deals with the design of the corrugated AVA. Section IV covers the design and analysis of corrugated AVA with the novel metamaterial unit cells. The simulated results of the proposed AVA are discussed in Section V. The outcomes of the proposed AVA are concluded in Section VI, followed by references.

II. DESIGN OF CONVENTIONAL AVA (CAVA)

Antipodal Vivaldi Antenna (AVA) was first proposed by Gazit in 1988. It unveils superior features such as wideband, high gain, stable radiation pattern and easy fabrication and hence it can efficiently gratify the various requirements of SATCOM. It consists of tapered or exponential metallic patches on top and bottom plane with a microstrip feed line matching with the connector, as shown in Figure 1.

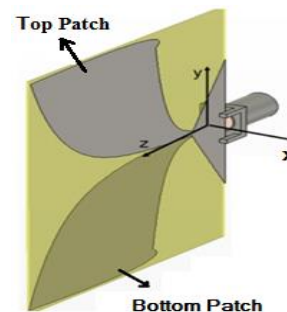


Figure 1. Antipodal Vivaldi Antenna [8]

Figure 2 depicts the geometry of the Conventional Antipodal Vivaldi Antenna (CAVA) simulated in HFSS ver. 13. This antenna consists of two parts: elliptical curved radiation flares and feed line. The top and bottom patches act as radiator and ground respectively. The antenna is designed on standard and economical substrate FR4 with a dielectric constant of 4.4, $\tan \delta$ as 0.02 and thickness 1.6 mm and simulated using HFSS ver. 13. As the Antipodal antennas operate as a resonant antenna at the lower end of frequency band, the antenna length L_1 and width W_1 is determined based on the lowest frequency f_L , relative dielectric constant ϵ_r . The antenna dimensions are calculated by using the following equations [8]:

$$L_1 = \frac{c}{f_L} \sqrt{\frac{2}{\epsilon_r + 1}} \quad (1)$$

$$W_1 = \frac{c}{2f_L \sqrt{\epsilon_r}} \quad (2)$$

The curve equations are given as

$$Y = \pm(R_1 e^{rx} + R_2) \quad (3)$$

Where R1 and R2 are given by:

$$R_1 = \frac{y_2 - y_1}{e^{rx_2} - e^{rx_1}} \quad (4)$$

$$R_2 = \frac{e^{rx_2} y_1 - e^{rx_1} y_2}{e^{rx_2} - e^{rx_1}} \quad (5)$$

Here, R1 and R2 are constants, 'r' symbolizes the increase rate of an exponential curve and, x1, y1, are the initial points and x2, y2 are the termination points of the exponential curve.

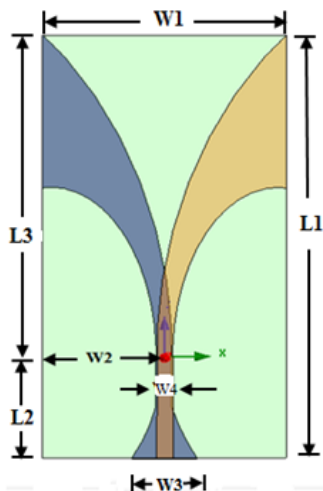


Figure 2. Structure of CAVA

The dimensions of the CAVA are calculated to have an optimized response over the desired bandwidth and they are found to be as follows: L1= 22.60 mm, L2 = 5.50 mm, L3= 17.1 mm, W1= 15.8 mm, W2= 7.2 mm, W3= 4.2 mm. The width of the microstrip feedline (W4) is calculated to match the characteristic impedance of 50 ohm which comes out to be W4= 1.25 mm. The radiating structure of the antenna is formed from the intersection of quarters of two ellipses, as explained in [9].

Figure 3 depicts the S11 response for the CAVA. From the curve, it can be seen that the designed CAVA resonates below -10 dB in the range of 10.8 GHz to more than 25 GHz. Figure 4 shows that CAVA achieves low gain at lower frequencies with maximum gain of 5.8 dBi only.

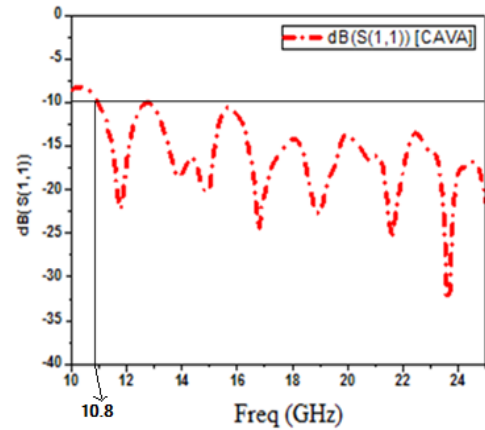


Figure 3. Frequency response of CAVA

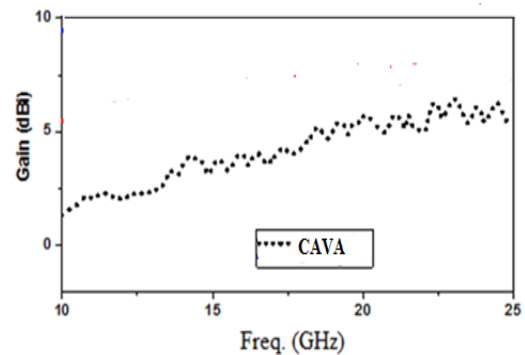


Figure 4. Gain plot of CAVA

Since the proposed CAVA dispenses low gain at lower frequencies, corrugation can be used to overcome this problem [10]. This will be explained in detail in Section III.

III. DESIGN OF CORRUGATED AVA

The low frequency performance of an AVA flare is enriched by the corrugation on its outer edges. Figure 5 depicts the design of the equilateral triangular corrugated AVA with slot side length, $S = 0.85$ mm.

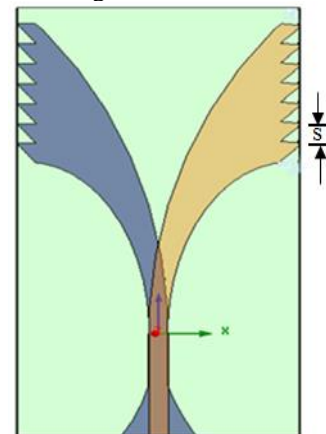


Figure 5. Structure of Corrugated AVA

The simulated S11 response of corrugated AVA is depicted in Figure 10. It can be seen that by adding corrugation, the lower cutoff frequency shifts to 10.3 GHz. The reason behind this shift in frequency is that the slot corrugation facilitates the electrical length of the inner taper profile to be elongated thereby extending the lower end cut-off frequency [11]. Further, the corrugation acts as a high impedance region due to which the maximum surface current remains towards the inner edge of the tapered slot reducing side and backlobe radiation, increasing the gain in boresight direction [12].

To further enhance the gain and improve the radiation characteristics, an array of metamaterial is commonly used on AVA aperture [13]. This will be explained in detail in Section IV.

IV. DESIGN AND ANALYSIS OF CORRUGATED AVA WITH METAMATERIAL (MTM)

To enhance the gain and characteristics of the proposed Vivaldi antenna, an array of epsilon negative metamaterial (ENG) unit cells is supplemented at its aperture. The proposed ‘pi shape (π)’ metamaterial is shown in Figure 6. The proposed MTM is placed inside a waveguide with Perfect Magnetic Conductors (PMC) on its top and bottom, Perfect Electric Conductors (PEC) on its side walls and two waveguide ports for excitation, as shown in Figure 7. Standard retrieving procedure is followed by using transmission and reflection coefficient of the unit cell, as described in [14], and it is found that the proposed metamaterial unit cell exhibits epsilon negative property, as shown in Figure 8. The optimized dimensions (in mm) of unit cell are as follows: A = 1.6, B = 0.25, C = 1.35, D = 0.70

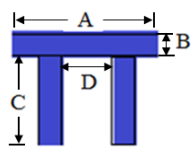


Figure 6 π shape Metamaterial Unit Cell

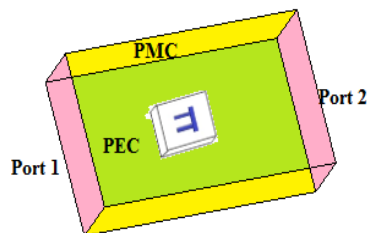


Figure 7. Simulation model of the proposed unit cell

Figure 8 illustrates the ENG behaviour of the unit cell with negative relative permittivity property in range of 14 GHz - 18 GHz.

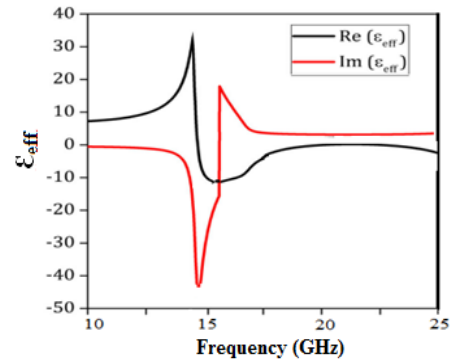


Figure 8. Permittivity graph of ENG unit cell

The MTM array was supplemented to the upper side of the antenna radiating aperture to augment the performance of the corrugated AVA. Using [15] and analysing by various placements and numbers of the proposed metamaterial cells for the desired frequency range, it was found that the proposed design with six MTM cells at 3-2-1 arrangement (from the top), as shown in Figure 9, attains the preferred bandwidth with better gain radiating maximum energy in the end-fire direction, as will be discussed in Section V.

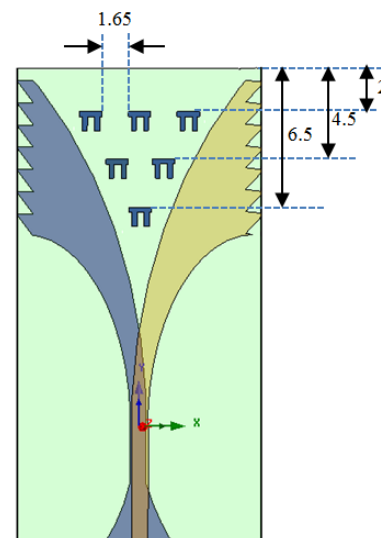


Figure 9. Corrugated AVA with Metamaterial (MTM) unit cells

V. RESULTS AND DISCUSSION

Figure 10 illustrates the simulated results of reflection coefficient (S11) with frequency for the corrugated AVA and corrugated MTM AVA. As can be noticed from the figure, the reflection coefficient of the corrugated AVA is below -10 dB for the frequency range of 10.3 GHz to 25 GHz. Applying the corrugation technique resulted in extension of the lower end frequency limit due to elongation of inner taper length. The negative index metamaterial

further ameliorated the lower cut-off frequency making $S_{11} < -10$ dB for the entire range from 10 GHz - 25 GHz.

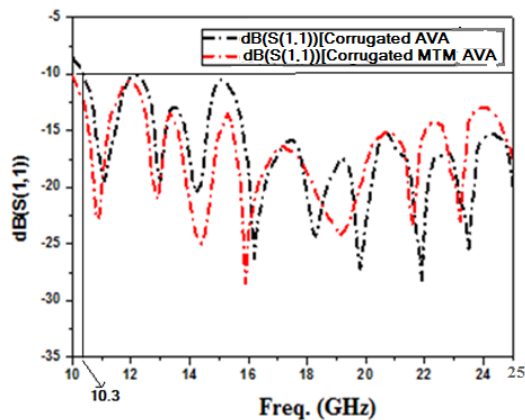


Figure 10. Comparison of Frequency response of Corrugated AVA and Corrugated MTM AVA

Figure 11 depicts the comparison of the gain plot of Corrugated AVA and Corrugated MTM AVA. The Corrugated AVA provides gain in the range of 6.5 dBi - 8.6 dBi, whereas the AVA-M provides the gain in the range of 7.3 dBi - 12.2 dBi with maximum gain achieved at 14.5 GHz. As evident from the gain plot, by integrating corrugation on both side edges of conducting arms, the gain of the proposed antenna increased significantly, especially at the lower end of the operating frequency band. Further, by integrating the metamaterial unit cells structure, the gain enrichment is more pronounced in the mid frequency band. Hence, the peak gain is enhanced by approximately 3.8 dBi in the desired range after inclusion of metamaterial unit cells, which is a significant gain enhancement without changing the antenna size.

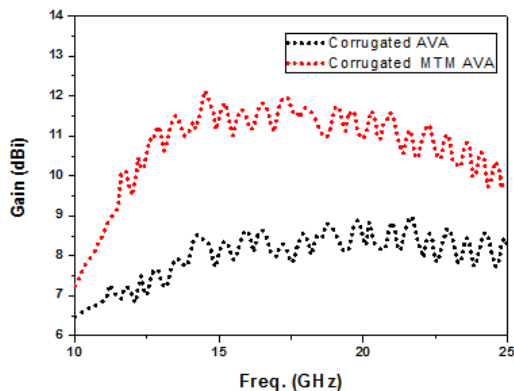


Figure 11. Comparison of Gain of Corrugated AVA and Corrugated MTM AVA

Figure 12 and Figure 13 illustrate the radiation patterns of the corrugated AVA and the proposed MTM antenna on the E-plane and H-plane at 10, 15 and 25 GHz, respectively.

It can be seen from the radiation pattern that loaded MTMs result in better directivity with improvement in gain [16] and possess enhanced radiation performance by suppressing the undesired side lobes [17] resulting in low side lobe levels.

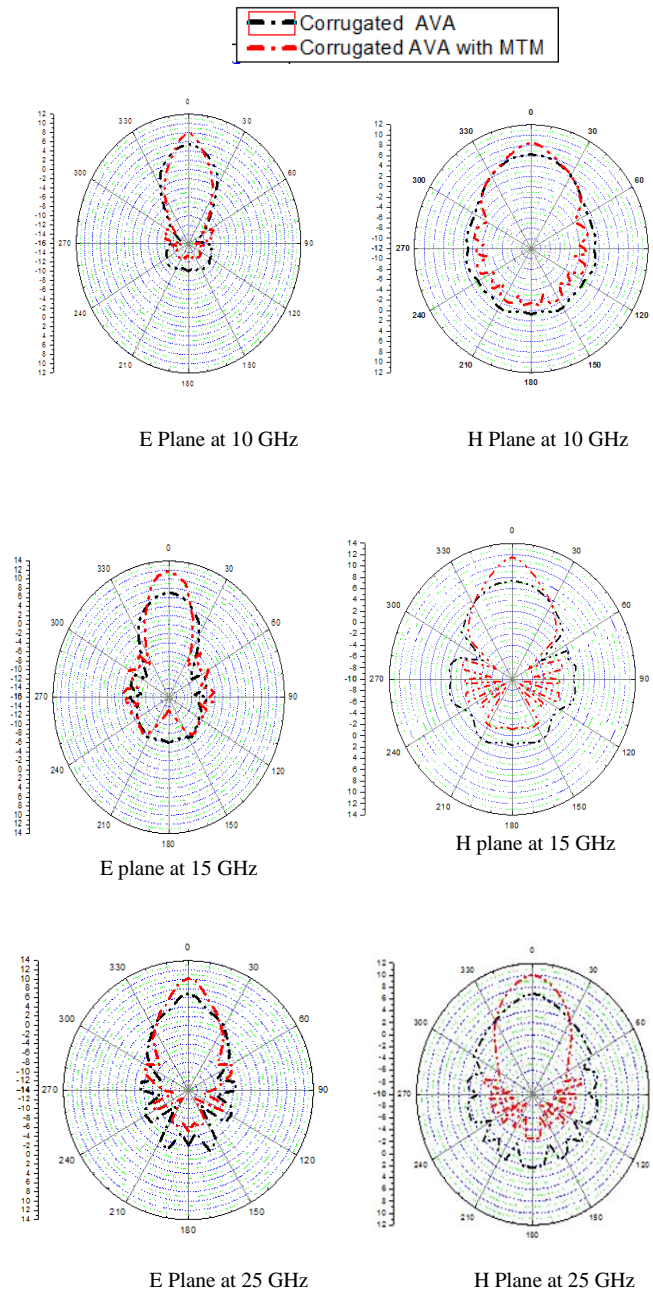


Figure 12. E plane radiation patterns

Figure 13. H plane radiation patterns

As it is evident that the proposed antenna offers higher directivity, but it can be costlier due to the complex fabrication process.

VI. CONCLUSION

This paper proposes the design and analysis of a high gain corrugated AVA with novel epsilon negative (ENG) metamaterial. The ENG metamaterial enhances the reflection coefficient with a wider bandwidth from 10 to 25 GHz without increasing the size. Further, the proposed corrugated MTM AVA enhances the gain by approximately 3.8 dBi as compared to corrugated AVA in the desired frequency range. As the proposed AVA design provides enhanced gain, improved return loss and compactness, it can be considered as a suitable candidate for satellite transmitter applications.

ACKNOWLEDGMENT

This work was undertaken during the tenure of an “ERCIM (The European Research Consortium for Informatics and Mathematics) Alain Bensoussan Fellowship” programme. Founded in 1988, ERCIM has members from leading European information technology and mathematics research establishments from 18 countries, with its head office in France.

REFERENCES

- [1] K. -X. Li, Z. -J. Guo and Z. -C. Hao, "A Multipolarized Planar Phased Array for LEO SATCOM Applications," in *IEEE Antennas and Wireless Propagation Letters*, vol. 21, no. 11, pp. 2273-2277, Nov. 2022.
- [2] N. Muchhal, M. Elkhoully, K. Blau and S. Srivastava, "Design of Highly Selective Band-pass Filter with Wide Stop-band using Open Stubs and Spurlines for Satellite Communication (SATCOM) Applications", *The Fourteenth International Conference on Advances in Satellite and Space Communications, SPACOMM 2022, April 2022, Barcelona, Spain.*
- [3] P. J. Gibson, "The Vivaldi Aerial," 1979 9th European Microwave Conference, 1979, pp. 101-105.
- [4] E. Gazit, "Improved design of the Vivaldi antenna", *IEE Proceedings H-Microwaves, Antennas and Propagation*, vol. 135(2), pp. 89–92, 1988.
- [5] I. T. Nassar and T. M. Weller., "A novel method for improving antipodal Vivaldi antenna performance", *IEEE Transactions on Antennas and Propagation*, 63(7), pp. 3321–3324, 2015.
- [6] M. Moosazadeh, S. Kharkovsky, and J. T Case, "Microwave and millimetre wave antipodal Vivaldi antenna with trapezoid-shaped dielectric lens for imaging of construction materials", *IET Microwaves, Antennas & Propagation*, 10(3), pp. 1–9, 2015.
- [7] A. S. Dixit and S. Kumar, "A miniaturized antipodal vivaldi antenna for 5G communication applications" 7th international conference on signal processing and integrated networks (SPIN), pp. 800-803, 2020.
- [8] S. Wang, X. D. Chen and C. G. Parini, "Analysis of Ultra Wideband Antipodal Vivaldi Antenna Design," 2007 Loughborough Antennas and Propagation Conference, Loughborough, UK, 2007, pp. 129-132.
- [9] A. M. Abbosh, H. K. Kan, and M.E Bialkowski, "Design of compact directive ultra-wideband antipodal antenna", *Microwave and Optical Technology Letters*, pp. 2448-2450, vol. 48, issue 12, Dec. 2006.
- [10] A. S. Dixit and S. Kumar, "A Survey of Performance Enhancement Techniques of Antipodal Vivaldi Antenna," in *IEEE Access*, vol. 8, pp. 45774-45796, 2020.
- [11] J. Bai, S. Shi, and D.W. Prather, "Modified compact antipodal Vivaldi antenna for 4–50 GHz UWB application". *IEEE Trans. Microw. Theory Tech.* 59(4), pp. 1051–1057, 2011.
- [12] Gaurav Kumar Pandey, Manoj Kumar Meshram, "A printed high gain UWB vivaldi antenna design using tapered corrugation and grating elements", *International Journal of RF and Microwave Computer-Aided Engineering*, pp. 610-618, vol. 25 (7), September 2015.
- [13] A. S. Dixit and S. Kumar, "The enhanced gain and cost-effective antipodal Vivaldi antenna for 5G communication applications", *Microwave and Optical Technology Letters*, pp. 2365-2374, vol. 62 (6), 2020.
- [14] N. Muchhal, S. Srivastava, and M. Elkhoully, "Analysis and Design of Miniaturized Substrate Integrated Waveguide CSRR Bandpass Filters for Wireless Communication", in *Recent Microwave Technologies*. London, United Kingdom: IntechOpen, 2022.
- [15] M. Guo, R. Qian, Q. Zhang, L. Guo, Z. Yang, and Z.Wang, "High-gain antipodal Vivaldi antenna with metamaterial covers", *IET Microwaves, Antennas & Propagation*, p. 2654-2660, vol. 13, issue 15, 2019.
- [16] L Chen, Z Lei, R Yang, J Fan, X Shi. "A broadband artificial material for gain enhancement of antipodal tapered slot antenna", *IEEE Trans. Antennas Propag.* 63(1): pp. 395-400, 2015.
- [17] M. C. Johnson, S. L. Brunton, N. B. Kundtz and J. N. Kutz, "Sidelobe Canceling for Reconfigurable Holographic Metamaterial Antenna," in *IEEE Transactions on Antennas and Propagation*, vol. 63, no. 4, pp. 1881-1886, April 2015.